Proceedings of the 2000 IEEE
International Conference on Robotics & Automation
San Francisco, CA • April 2000

A Whisker Tracing Sensor with 5μm Sensitivity

Makoto Kaneko and Toshio Tsuji

Industrial and Systems Engineering
Hiroshima University
Kagamiyama, Higashi-Hiroshima 739-8527, JAPAN

Abstract

This paper discusses a whisker sensor composed of a flexible beam anchored at the base with torque sensor, and an actuator for moving it. We consider a sufficient condition for detecting the surface shape by using a whisker sensor. We show that a straight-lined whisker sensor with one axis torque sensor can achieve the requirement irrespective of contact friction, while a curved whisker can not do it. We experimentally show that a straight-lined whisker sensor can detect the surface irregularity with pretty high sensitivity ($\leq$ 5 [μm]), even under different contact frictions.

Key words: *Whisker Sensor, High Sensitivity, Surface Probing, Surface Tracing, Burr Detection*

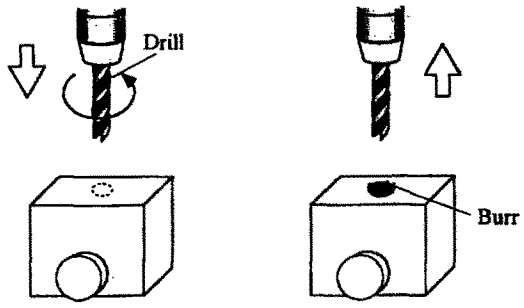

(a) Before drilling (b) After drilling

Fig. 1: An example where burrs appear

1 Introduction

Why whisker sensor?
Before assembling, each mechanical part is finished through various machining process, such as cutting, welding, pressing, lathing, reaming, and drilling. After either reaming or drilling process, we can often find burrs, as shown in Fig.1. Such burrs may bring a serious problem when the part is sent to the assemble line without removing them. For example, suppose that the part is assembled in a hydraulic system including valves with extremely small ports. Once a piece of burr is detached due to pressure disturbance during operation, it will start to move around the fluid circuit. This may finally block the port of the valve and lead to the system down as the worst scenario. A deburring tool is often utilized after drilling, so that we can completely remove burrs. Nevertheless, it is hard to perfectly remove all burrs and there is a small chance where a piece of burr still remains unremoved. Therefore, it is necessary to monitor whether burrs are completely removed from the finished surface or not.

For detecting burrs, there are two approaches, namely, non-contact based and contact based sensing. Vision is a popular and powerful sensor categorized in non-contact sensing group. By using an optical fiber, it can extract a scene where burrs exist, even though they are located around a small hole. However, since it is strongly influenced by lighting condition, it may fail in recognizing burrs when they are small enough or they provide with mirror reflecting like image. While a laser based sensor as shown in Fig.2(a) can supply high sensitivity, the sensor head (120 [mm]) is not sufficiently small to make it possible to insert the head into a small hole. On the other hand, our finger can easily feel the sensation of irregularities on surface, even though they are just a few micrometers and hard to be recognized by our eyes. This suggests the superiority of tactile sensing to vision in human especially when the object is extremely small. Considering such an advantage of tactile sensing, we focus on tactile probe in this work.

As for tactile probe, an electric type dial gauge as shown in Fig.2(b) is commercially available with an economical price. While the resolution ($\leq$ 2 [μm]) is more than enough for our purpose, the problem is that the sensor head ($\geq$ 10 [mm]) is still too large to be inserted into a small hole. Therefore, it is not appropriate for applying the burr detection. While a number of other tactile sensors have been proposed for reconstructing the surface of environment, we are particularly interested in using a whisker type sensor because of its flexibility and slender shape. The flexibility of whisker releases us from fixing mechanical parts to be examined with the exactly designated position, since the whisker can adapt to some extent by itself. The flexibility is also effective for avoiding any damage to mechanical parts while the whisker is contacting them.

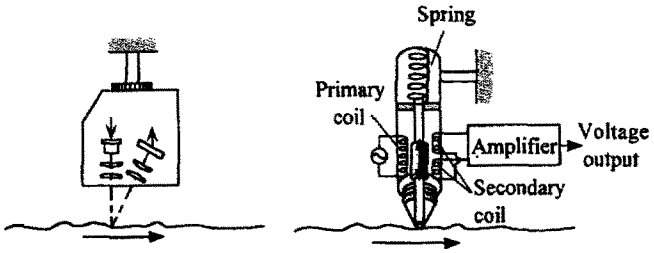

(a) An example of laser distance sensor

(b) An example of electric dial gauge

Fig. 2: Two examples of non-contact and contact based sensing

Goal of this work
Knowing of the necessity of a whisker sensor, our goal is to answer the following questions. (1) Can a whisker sensor with torque sensors always reconstruct the surface irregularity? (2) If this is not the case, under what condition it can achieve it? (3) If this is the case, how accurately it can reconstruct the surface shape? While there have been various works on whisker sensor, so far, no work can answer for these questions. After briefly reviewing conventional works, we consider a sufficient condition for a whisker sensor to detect a surface shape and show that a straight-lined whisker sensor with one axis torque sensor can detect the surface shape irrespective of the contact friction, while a curved whisker can not achieve it under one axis moment sensor. Through experiments, we verify that even a straight whisker sensor can detect surface irregularities with pretty high sensitivity (≤ 5 [μm]). We also show an experimental result where a whisker sensor is applied as a burr detection sensor.

2 Related Works

A simple flexible beam sensor can take the form of a short length of spring piano wire or hypodermic tubing anchored at the end. When the free end touches an external object, the wire bends and this can be sensed by a piezoelectric element or by a simple switch [1]. A more elaborate sensor is described by Wang and Will [2]. Long antennae-like whisker sensors were mounted on the SRI mobile robot Shakey [3] and on Rodney Brock's six-legged robot insects [4]. Hirose and others discussed the utilization of whisker sensors in legged robots [5]. The sensor system is composed of an electrode and a whisker whose end is fixed at the base. This sensor unit has been arranged in an array around each foot of the legged robot, TITAN III, so that it can monitor the separation between each foot and the ground. This sensor is also conveniently used to confirm which part of the foot is in contact with the ground. Similarly shaped whisker have been considered for legs of the Ohio State University active suspension vehicle [6]. Russell has developed a sensor array [7] and succeeded in reconstructing the shape of convex object followed by the whisker. Wilson and Mahajan [8], Snyder and Wilson [9] have designed the whisker probe system composed of a piano wire with strain gauge sensors and the base sweep actuators made of two polyurethane tubes that bend when pressurized with air. Wilson and Chen [10] have reported experimental results that demonstrate the precision and accuracy of the whisker probe system in detecting and displaying solid boundaries enclosing areas up to 40 by 50 [cm]. These works assume that the whisker tip always makes contact with the object. Kaneko, Kanayama and Tsuji [11] have proposed the Active Antenna that can localize a contact point between a flexible beam and environment through a pushing motion. Tsujimura and Yabuta have addressed an object shape detection system using a force/torque sensor and an insensitive flexible probe [12].

3 Can a Whisker Sensor Detect Surface Shape?

Now, let us consider a general whisker model as shown in Fig.3, where $\tau = (\tau_x, \tau_y, \tau_z)^t \in R^{3\times1}$, $M = (m_x, m_y, m_z)^t \in R^{3\times1}$, and $f = (f_x, f_y, f_z)^t \in R^{3\times1}$ are torque at the base, moment and force at the tip of the beam, respectively. For simplifying our discussion, we set the following assumptions.

Assumption 1: The deformation of whisker is small enough to ensure that we can apply classical beam theory.
Assumption 2: The elongation of a straight-lined whisker due to a unit axial force is negligibly small compared with the deflection due to a unit bending force.
Assumption 3: The whisker tip (or close to the tip) always makes contact with the environment to be sensed.

Assumption 1 guarantees the following linear relationship between force(moment) and displacements.

$$\begin{bmatrix} d\delta \\ d\theta \end{bmatrix} = \begin{bmatrix} D_{11} & D_{12} \\ D_{21} & D_{22} \end{bmatrix} \begin{bmatrix} f \\ M \end{bmatrix} \quad (1)$$

where $d\delta = [\delta_x, \delta_y, \delta_z]^t \in R^{3\times1}$, $d\theta = [d\theta_x, d\theta_y, d\theta_z]^t \in R^{3\times1}$, $D_{ij} \in R^{3\times3} (i = 1,2; j = 1,2)$ denote the displacement vector, the angular displacement vector, the block compliance matrix, respectively. Since we can generally neglect the moment M at the contact point, we can focus on the relationship between $d\delta$ and f.

$$d\delta = D_{11} f \quad (2)$$

Additionally, we have the following relationship between τ and f.

$$\tau = J^t f \quad (3)$$

where J^t is the Jacobian matrix mapping from f to τ. We now examine whether $d\delta$ can be estimated by measuring τ. Suppose that there are three torque sensing

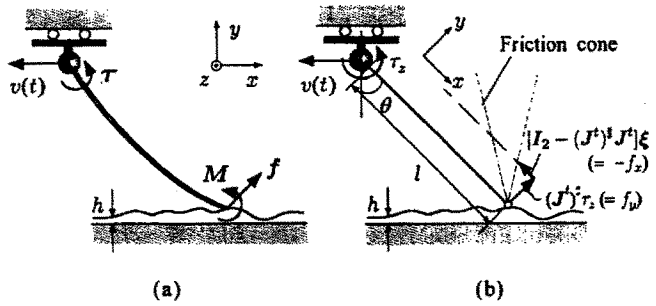

Fig. 3: Analytical model of whisker sensor

axes around x, y, z, respectively. Since $\boldsymbol{J}^t \in R^{3\times 3}$ under such an assumption, the inverse of $\boldsymbol{J}^t$ exists if $det\left|\boldsymbol{J}^t\right| \neq 0$.

$$d\boldsymbol{\delta} = \boldsymbol{D}_{11}[\boldsymbol{J}^t]^{-1}\boldsymbol{\tau} \tag{4}$$

Therefore, we can estimate $d\boldsymbol{\delta}$ through the measurement of $\boldsymbol{\tau}$. Now, we consider whether a fewer numbers of torque sensors can successfully estimate the displacement(or height) or not. Suppose that only z-axis torque sensor is available. This component can be picked up by multiplying a selection vector $\boldsymbol{s} = (0,0,1)^t$ for eq.(3). Namely,

$$\boldsymbol{s}^t\boldsymbol{\tau} = \boldsymbol{s}^t\boldsymbol{J}^t\boldsymbol{f} \tag{5}$$

where $\tau_z = \boldsymbol{s}^t\boldsymbol{\tau}$. Under the assumption, we have the following relationship,

$$\boldsymbol{f} = (\boldsymbol{J}_1^t)^\sharp\tau_z + [\boldsymbol{I}_3 - (\boldsymbol{J}_1^t)^\sharp\boldsymbol{J}_1{}^t]\boldsymbol{\xi} \tag{6}$$

where $\boldsymbol{J}_1{}^t = \boldsymbol{s}^t\boldsymbol{J}^t$, $\boldsymbol{I}_3 \in R^{3\times 3}$, $\boldsymbol{\xi} \in R^{3\times 1}$, and $\sharp$ denote the Jacobian matrix from $\boldsymbol{f}$ to τ_z, the unity matrix, an arbitrary vector, and seudo-inverse matrix, respectively. The first term of $\boldsymbol{f}$ is the force component that can be measured by the torque sensor and the second term is the one that can not be evaluated by the sensor. Eq.(6) means that the contact force $\boldsymbol{f}$ can not be uniquely determined for a measured torque τ_z. In other words, the force component $[\boldsymbol{I}_3 - (\boldsymbol{J}_1^t)^\sharp\boldsymbol{J}_1^t]\boldsymbol{\xi}$ perpendicular to $(\boldsymbol{J}_1^t)^\sharp\tau_z$ varies depending upon the friction at point of contact. Substituting eq.(6) into eq.(2), we obtain

$$d\boldsymbol{\delta} = \boldsymbol{D}_{11}(\boldsymbol{J}_1{}^t)^\sharp\tau_z + \boldsymbol{D}_{11}[\boldsymbol{I}_3 - (\boldsymbol{J}_1^t)^\sharp\boldsymbol{J}_1{}^t]\boldsymbol{\xi} \tag{7}$$

Due to the existence of a null space in eq.(7), in general, we can not uniquely determine $d\boldsymbol{\delta}$ through the measurement of τ_z alone.

4 Is There Any Case Where the Null Space Disappear?

Let us consider a straight lined whisker as shown in Fig.3(b), where the whisker is slightly pressed on the surface and the inclined coordinate system is considered for simplifying the discussion. Note that if the displacement is assumed to be the order of 100 [μm], we can regard that the beam with the length of a few centimeters still keeps a straight line even under such a pressed phase. For such a 2D model, $\boldsymbol{D}_{11}$ and $\boldsymbol{J}_1{}^t$ are given by

$$\boldsymbol{D}_{11} = \begin{pmatrix} \frac{l}{EA} & 0 \\ 0 & \frac{l^3}{3EI} \end{pmatrix}, \quad \boldsymbol{J}_1{}^t = (0, l) \tag{8}$$

where l, E, A, and I are the beam length, the elasticity, the cross sectional area, and the second order moment of cross section of the beam, respectively. Substituting eq.(8) into $\boldsymbol{D}_{11}(\boldsymbol{J}_1{}^t)^\sharp\tau_z$ and $\boldsymbol{D}_{11}[\boldsymbol{I}_2 - (\boldsymbol{J}_1{}^t)^\sharp\boldsymbol{J}_1{}^t]\boldsymbol{\xi}$, we obtain

$$\begin{aligned} \boldsymbol{D}_{11}(\boldsymbol{J}_1^t)^\sharp\tau_z &= \begin{bmatrix} \frac{l}{EI} & 0 \\ 0 & \frac{l^3}{3EI} \end{bmatrix}\begin{bmatrix} 0 \\ l \end{bmatrix}\tau_z \\ &= \begin{bmatrix} 0 \\ \frac{\tau_z l^2}{3EI} \end{bmatrix} \end{aligned} \tag{9}$$

$$\begin{aligned} \boldsymbol{D}_{11}[\boldsymbol{I}_2 - (\boldsymbol{J}_1^t)^\sharp\boldsymbol{J}_1{}^t]\boldsymbol{\xi} &= \begin{bmatrix} \frac{l}{EA} & 0 \\ 0 & \frac{l^3}{3EI} \end{bmatrix}\begin{bmatrix} 1 & 0 \\ 0 & 0 \end{bmatrix}\begin{bmatrix} \xi_1 \\ \xi_2 \end{bmatrix} \\ &= \begin{bmatrix} \frac{l\xi_1}{EA} \\ 0 \end{bmatrix} \end{aligned} \tag{10}$$

During a tracing motion, the contact force may appear on either boundary of the friction cone. Therefore, ξ_1 can not be an infinite value, and is limited as shown in Fig.3(b). For such a limited force, classical beam theory ensures that the longitudinal deflection $l\xi_1/EA$ is even smaller than the bending deformation $\tau_z l^2/3EI$ (Assumption 2). Thus, the displacement caused by the force in null space can be neglected. As a result, we can estimate the surface height h uniquely by

$$h = \delta_y \sin\theta = \frac{\tau_z l^2}{3EI}\sin\theta \tag{11}$$

It should be noted that there exists one to one mapping between h and τ_z, even though a friction force makes the contact force shift within the null space.

[Remark]
Surface irregularities are observable under a straight-lined whisker with one-axis torque sensor, irrespective of the contact friction.

This is a great advantage for using a straight lined whisker, while we can not keep such robustness against friction under the utilization of a curved beam.

5 How should We Consider Dynamic Effect?

Hereafter, we assume a straight-lined whisker sensor with one-axis torque sensor and a surface with 2D irregularities, so that we can focus on 2D problem. As the tracing speed increases, dynamic effect will become dominantly. Such a dynamic effect produces

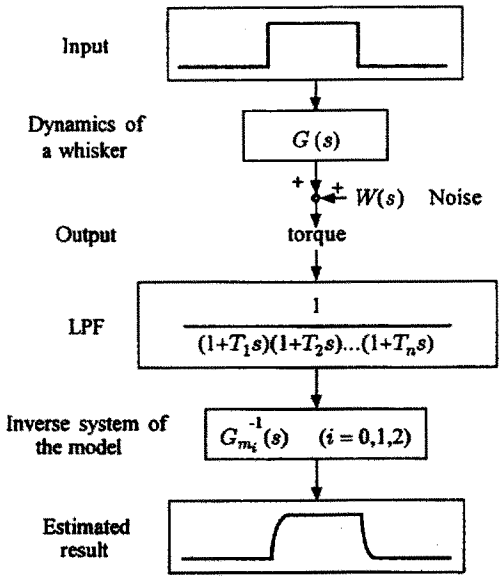

Fig. 4: Data processing flow

mechanical vibration over the whisker and, as a result, vibration signals are also observed from the output of strain gauge in addition to a static drift. Under such dynamics effects, the relationship between input and output is expressed in the following,

$$T(s) = G(s)H(s) + W(s) \tag{12}$$

where $T(s)$, $H(s)$ and $W(s)$ are Laplace transformation of torque, the height from the base, and noise, respectively, and $G(s)$ is the transfer function between $H(s)$ and $T(s)$.

$W(s)$ can be removed by using an appropriate filter. Therefore, if $G(s)$ is given, we can obtain the height with respect to time,

$$h(t) = \mathcal{L}^{-1}\{G^{-1}(s)T(s)\} \tag{13}$$

where $\mathcal{L}^{-1}\{\cdot\}$ denotes the inverse of Laplace transformation. The signal processing for obtaining $h(t)$ is shown in Fig.4, where the Low-Pass Filter(LPF) is indispensable so that the inverse system may become proper. However, it is extremely difficult to obtain $G(s)$ in an exact form. No analytical formulation can be found in the literature treating flexible manipulators. Instead of using an exact form of $G(s)$, we utilize an approximated form $G_{mi}(i = 0, 1, 2)$, where G_{m0}, G_{m1} and G_{m2} are the model with a spring alone, the model incorporated with the fundamental natural frequencies, and the model with both the fundamental and second natural frequencies, respectively, and given by,

$$G_{m0} = k_1 \tag{14}$$

$$G_{m1} = \frac{{k_2}^2}{2k_1 + m_1 s^2} \tag{15}$$

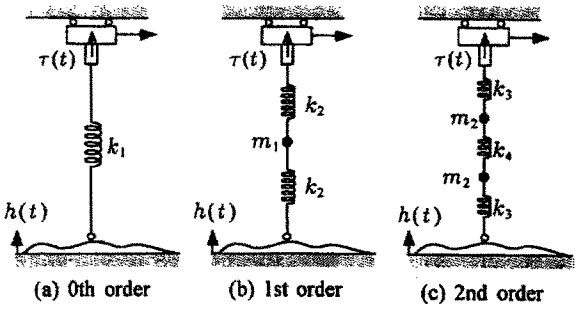

Fig. 5: Mass-spring model

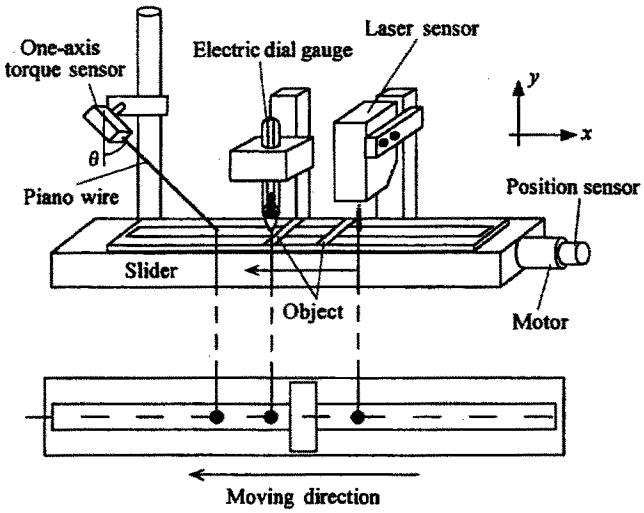

Fig. 6: Experimental system

$$G_{m2} = \frac{{k_3}^2 k_4}{(k_3 + m_2 s^2)(k_3 + 2k_4 + m_2 s^2)} \tag{16}$$

where $m_i(i = 1, 2)$ and $k_i(i = 1, 2, 3, 4)$ denote the mass and the spring, respectively, as shown in Fig.5. Without losing generality, the real system can be replaced by a simple mass-spring model, where m_i and k_i are chosen, in such a way that the natural frequencies between the real system and the model may coincide with those of the real whisker sensor in contact with the surface.

6 How Accurately a Whisker Sensor can Reconstruct Surface Shape?

Now, let us consider a simple whisker sensor, where a straight lined whisker is anchored with a base equipped with a strain gauge. An interesting question that comes up to us is *How accurately such a sensor can reconstruct the surface shape with irregularities?*

To examine the sensing capability, we developed a whisker sensor by using a piano wire whose the length and diameter are 100 [mm] and 1.4 [mm], respectively. The piano wire is connected with the base with a strain gauge. Through a vibration test, the fundamental and

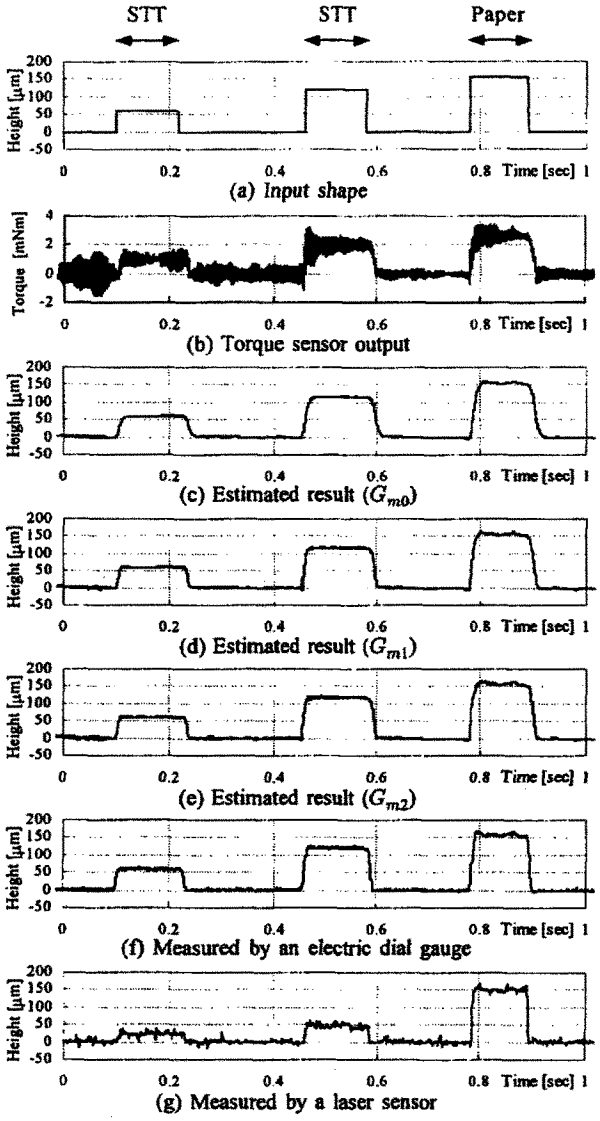

Fig. 7: An experimental result

second natural frequencies under contact with a surface are $f_1 = 374$ [Hz] and $f_2 = 1210$ [Hz], respectively. Fig.6 shows an experimental system where instead of moving the sensor, the surface is moved by the slider. A laser distance sensor as well as an electric dial gauge are also installed in the system for comparison. It is important to note that all sensors are placed in such a way that they may trace the same point as shown in Fig.6. In order to obtain the basic characteristic of the sensor, we prepare various materials for the surface, such as semi-transparent tape (STT), non-transparent tape (NTT), copy paper, and rubber. The contact friction is small for both STT and NTT, while it is not for paper and rubber. Fig.7 shows an experimental result for three different steps (60, 120, and 150 [μm]), where (a), (b), (c), (d), (e), (f), and (g) are the original input height, the output from the sensor without any filtering, the estimation

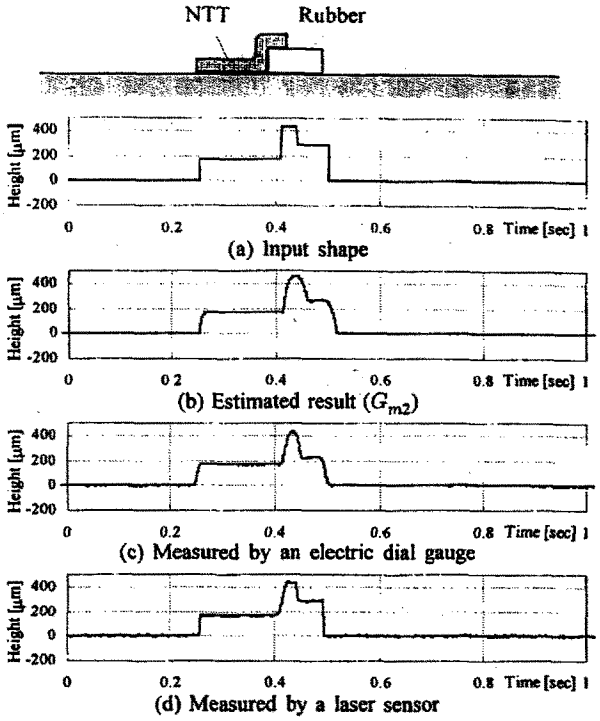

Fig. 8: An experimental result

results using G_{m0}, G_{m1}, and G_{m2}, the output from the electric dial gauge, and the output from the laser distance sensor, respectively, and the surface material used for each step is indicated in (a) with abbreviation form. Through this experiment we can see that the whisker sensor exhibits as high sensitivity as the electrical dial gauge with the sensitivity of less than 2 [μm]. Through more precise experiments, we found that the whisker sensor has less than 5 [μm] resolution even under conservative estimation. The surfaces reconstructed by using $G_{mi}(i = 1, 2, 3)$ are almost same over the flat surface but they have different responses in both step-up and step-down areas. Generally, we can expect a quicker response when we use G_{mi} with a higher order natural frequency. It should be noted that the laser distance sensor does not provide with an accurate height for a semi-transparent tape, while it can estimate a pretty accurate height for paper. This is because a part of light reflects on the top surface and the remaining on the bottom surface, when a semi-transparent tape is used as a surface. As a result, the laser sensor provides with an intermediate height between two surfaces. Fig.8 shows another experimental result where the irregular surface is made by a non-transparent tape and rubber, as shown in the top of Fig.8. The outputs from three sensors provide almost with the same height when the tip traces over the non-transparent tape, while they are different each other when the tip traces over the rubber. We note that the rubber is compliant. Therefore, it deforms while both whisker sensor and the dial gauge trace over the surface, through their direct contact with it. On the other hand, since the laser distance sensor is a non-

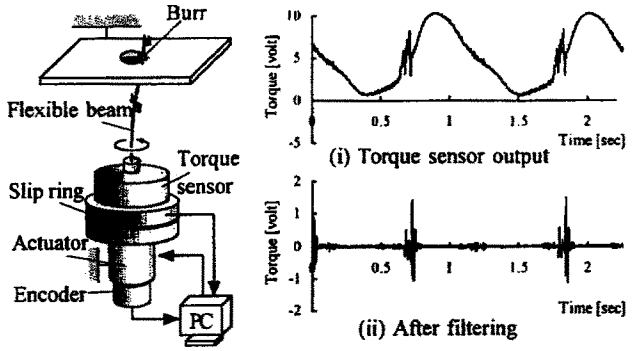

(a) Basic version (b) An experimental result

Fig. 9: Burr detection

contact sensor, it can provide the shape without any deformation. For such a compliant material, a tactile sensor generally provides a different shape depending on how much contact force is applied.

7 Application

Knowing of an excellent sensitivity of the simple sensor, we now discuss a burr detection sensor using a flexible beam. Fig.9(a) shows a general view of burr detection sensor where it is composed a flexible beam, an actuator for rotating it, an encoder for detecting the burr position, a rotational type torque sensor for detecting vibration signal caused by the contact between the beam and burrs, and a slip ring for exchanging electric signal between rotational and absolute systems each other. Generally, the output from the torque sensor $\tau(t)$ includes the following three signals,

$$\tau(t) = burr(t) + motor(t) + w(t), \qquad (17)$$

where $burr(t)$, $motor(t)$, and $w(t)$ are the signals arising from burrs, rotation of motor, and noise inherently including in torque sensor, respectively. If $burr(t)$, $motor(t)$, and $w(t)$ have their own frequencies and they are different each other, we can extract the signal brought by $burr(t)$ by applying an appropriate band-pass filter. Thus, we can pick up the vibration signal caused by burrs through an appropriate band-pass filter. These are the basic working principle of the burr detection sensor. Fig.9(b) shows an example of experimental data where (i) and (ii) are the original signal from the strain gauge and the output after the band-pass filter, respectively. We can see that the output from the band-pass filter includes the clear signal caused by burrs.

As far as burr detection is concerned, we are interesting to know whether there exists a burr or not, rather than how big it is. Therefore, the requested task is more easily achieved than that of surface reconstruction. As for the size of burr to be detected, the experiments in Chapter 6 ensure that the whisker sensor can detect the burr whose size is less than 5 [μm].

8 Concluding Remarks

We considered a whisker sensor and showed that a straight-lined whisker can successfully work as a surface reconstructing sensor with one-axis torque sensor alone, while a curved whisker can not. We also showed that the straight-lined whisker can detect a surface irregularities with the sensitivity of less than 5 [μm] under a conservative evaluation. We applied a whisker to a burr detecting sensor and confirmed the effectiveness. We believe that this type of whisker sensor can be applied to various fields where a slender sensor tip is especially required. Finally, the authors would like to express their thanks to Mr. Yoshiharu Bessho and Mr. Takefumi Mukai for their help for the experiments.

References

[1] R. A. Russel: Closing the sensor-computer-robot control loop, *Robot Age*, pp.15–20, Apr. 1984

[2] S. S. M. Wang and P. M. Will: Sensors for computer controlled mechanical assembly, *Ind. Robot*, pp. 9–18, Mar. 1978

[3] P. McKerrow: *Introduction to Robotics.* Reading, MA: Addison Wesley, 1990

[4] R. A. Brooks: A robot that walks; Emergent behaviors from a carefully evolved network, *Neural Computat.*, vol. 1, pp. 253–262, 1989

[5] S. Hirose *et al.*: Titan III, A quadruped walking vehicle, *Proc. 2nd Int. Symp. Robot Res.*, Cambridge, MA, 1985

[6] E. N. Schiebel, H. R. Busby, and K. J. Waldron: Design of a mechanical proximity sensor, *Robotica*, vol. 4, pp. 221–227, 1986

[7] R. A. Russel: Using tactile whiskers to measure surface contours, *Proc. 1992 IEEE Int. Conf. on Robotics and Automation*, pp. 1295–1300, 1992

[8] J. F. Wilson and U. Mhajan: The mechanics and positioning of highly flexible minipulator limbs, *ASME J. Mech., Transm., Automat. Des.*, vol. 111, pp. 230–237, 1989

[9] J. M. Snyder and J. F. Wilson: Dynamic of the elastica with end mass and follower loading, *ASME J. Appl. Mech.*, vol. 57, pp. 203–208, 1990

[10] J. F. Wilson and A. Chen: A whisker probe system for shape perception of solids, *ASME J. Dyn. Syst., Meas., Contr.*, vol. 117, pp. 104–108, 1995

[11] N. Kaneko, N. Kanayama and T. Tsuji: Active Antenna for contact sensing, *IEEE Trans. on Robotics and Automation*, vol. 14, no. 2, pp. 278–291, 1998

[12] T. Tsujimura and T. Yabuta: A tactile sensing method employing force/torque information through insensitive probes, *Proc. 1992 IEEE Int. Conf. on Robotics and Automation*, pp. 1315–1320, 1992